Wang, Z., Yang, M., Fu, L., Chen, C., You, R.*, and Ren, W.* 2020. Rapid field measurement of ventilation rate using a quartz-enhanced photoacoustic SF_6 gas sensor. ***Measurement Science and Technology,*** 31: 085105.

Rapid field measurement of ventilation rate using a quartz-enhanced photoacoustic SF_6 gas sensor

Zhen Wang[1,2,#], Min Yang[1,2,#], Liye Fu[3], Chun Chen[1], Ruoyu You[3,*], and Wei Ren[1,2,*]

[1]*Department Mechanical and Automation Engineering, The Chinese University of Hong Kong, New Territories, Hong Kong SAR, China*

[2]*Shenzhen Research Institute, The Chinese University of Hong Kong, New Territories, Hong Kong SAR, China*

[3]*Department of Building Services Engineering, The Hong Kong Polytechnic University, Kowloon, Hong Kong SAR, China*

[*]Corresponding: renwei@mae.cuhk.edu.hk (W. Ren); ruoyu.you@polyu.edu.hk (R. You).

[#]Contribute equally to this work.

Abstract:

We reported the development of a quartz-enhanced photoacoustic sulfur hexafluoride (SF_6) sensor for ventilation studies using a continuous-wave distributed-feedback quantum cascade laser (QCL) at 10.5 μm. The SF_6 sensor was developed by detecting the gas-absorption induced acoustic wave using a tiny quartz tuning fork that is enclosed in a gas cell with a sample volume of 2.5 mL. By locking the QCL wavelength at the absorption peak of SF_6, we obtained a recording time interval of 0.4 s and a detection limit of 4.6 ppb. The sensor response time (t_{90}) was found to be 2.8 s at a flow rate of 550 mL/min. The sensor was then implemented in measuring air exchange rates (AERs) in a laboratory room using the standard tracer gas concentration decay method. Our measurements are in good agreement with a commercial analyzer when studying two typical passive ventilation scenarios of infiltration and natural ventilation. Additionally, the developed photoacoustic gas sensor is fast enough to capture the transient variations of the SF_6 concentration during natural ventilation. This study provides a promising method of studying transient contaminant transport that remains a major challenge in air quality research.

Key words: Photoacoustic spectroscopy, ventilation rate measurement, sulfur hexafluoride tracer, optical gas sensor

1. Introduction

People spend most of their time indoors, so ventilation is of great significance to ensure a healthy and thermally comfort indoor environment for occupants to live and work [1]. Inadequate ventilation may lead to health threats such as sick building syndrome (SBS) and building-related illness (BRI) [2]. Monitoring ventilation rate, or air exchange rate (AER, defined by the ratio of the ventilation rate and space volume), is thus required by various standards and regulations for ventilation design and control [3,4]. In addition, computational fluid dynamics (CFD) has been widely used in the study of air quality in enclosed environments [5–7], as it is efficient and economic. As the validation of CFD calculations requires the measured ventilation rate as a boundary condition, the quantification of ventilation rates has become indispensable.

To determine the ventilation rate, one can employ the measured air velocities [8], pressure differences [9], and balances of heat, moisture, or carbon dioxide (CO_2) [10]. However, these techniques require the prior identification of locations of all openings, CO_2 or heat sources, which are at times impractical. Meanwhile, the intrusive feature of manometers and anemometers may influence the airflow patterns within the enclosed space [11]. Another promising method is the tracer gas technique, which provides a versatile and accurate alternative [8]. This technique is widely used to validate CFD models due to its non-destructive feature and the ability to be applied to occupied spaces and various ventilation systems [12]. By releasing a certain amount of tracer gas in the enclosure and measuring the concentration evolution with time, the AER can be obtained by the continuity equation [3]:

$$V\frac{dC}{dt} + (C - C_{atm}) \cdot N \cdot V = \dot{m} \quad (1)$$

where V (m^3) is the volume of the target enclosure, C ($kg \cdot m^{-3}$) is the tracer gas concentration at time t (s), C_{atm} ($kg \cdot m^{-3}$) is the tracer gas concentration in ambient air, N (h^{-1}) is the AER, and $\dot{m}$ ($kg \cdot h^{-1}$) is the total production rate of the tracer gas within the enclosure.

Among different tracer gases such as CO_2, nitrous oxide (N_2O), sulfur hexafluoride (SF_6) and Krypton-85 (^{85}Kr) [13], SF_6 is the most widely used stable gas that is non-harmful to occupants and scarcely present in ambient air. Commercially available instruments for SF_6 measurements include a gas chromatograph with an electron capture detector (GC-ECD) [14], non-dispersive

infrared sensors (NDIR) [15], and infrared gas analyzers [16]. GC has shortcomings of a long response time, a bulky size and a high cost, making it not suitable for real-time field tests. NDIR suffers from low sensitivity, poor selectivity and instability. In contrast, laser-based infrared spectroscopy is advantageous for real-time and *in situ* gas concentration measurements with high sensitivity and selectivity. Particularly, photoacoustic spectroscopy (PAS) employs a low-cost microphone for laser absorption-induced acoustic detection [17]. By performing intensity or frequency modulation of the laser source, the acoustic signal produced by the interaction between the modulated laser radiation and the target gas is detected by the microphone. Commercial SF_6 monitors based on infrared PAS such as INNOVA 1312 and Bruel & Kjaer (B&K) 1302 are currently the most prevalent instruments for ventilation measurements [6]. However, these commercialized SF_6 sensors have a relatively long response time up to tens of seconds, which are sometimes inadequate for measuring transient processes.

Quartz-enhanced photoacoustic spectroscopy (QEPAS) is one of the most sensitive gas sensing techniques [18–22]. The key feature is to use a quartz tuning fork (QTF) instead of a microphone for acoustic wave detection. The high quality factor (Q-factor ~ 10000 at atmospheric pressure) and high resonant frequency (~ 32.75 kHz) of a tiny QTF (Φ 3×8 mm) enables the ultrasensitive trace gas detection and an ultra-small sampling volume (i.e., 2.5 mL in this work) of the sensor system [23]. The measurement is normally performed by slowly scanning the laser wavelength across the target spectral feature. The sensor response time is limited by the scanning frequency at sub-Hz due to the use of a high Q-factor QTF [24]. Considering the necessity to know the transient change of the tracer gas, the wavelength stabilization method using the third harmonic (3f) as the error signal to lock the laser wavelength to the target absorption line is preferred over the commonly used scanned-wavelength method [25–27]. Other wavelength locking techniques using the phase variation of the photoacoustic signal [28] and the second harmonic (2f) signal [29] have also been successfully implemented in photoacoustic spectroscopy.

In this work, we focus on the development of a fast-response QEPAS-based SF_6 sensor at atmospheric pressure for ventilation rate measurements. A continuous-wave (cw) distributed-feedback quantum cascade laser (DFB-QCL) near 10.5 μm is used as the light source for SF_6 detection. The wavelength stabilization technique is implemented to lock the laser wavelength

at the absorption peak of SF_6. To evaluate and validate the sensor performance, the ventilation rate tests are performed in a laboratory room to measure both the infiltration and the natural ventilation. Our measurements are compared with the commercial SF_6 gas monitor (B&K 1302) to demonstrate the superiority of the QEPAS-based SF_6 sensor.

2. Sensor configuration and method

Figure 1 depicts the absorption coefficient of 1 ppm SF_6 between 900 cm^{-1} (11.1 µm) and 960 cm^{-1} (10.4 µm) based on the HITRAN database [30]. In general, SF_6 has a broad rovibrational absorption spectrum in the ν_3 fundamental band near 10.5 µm. The peak absorption appears at 947.89 cm^{-1} which could be accessed by commercial DFB-QCLs. As water is the major possible interference in ambient air, the simulated absorption coefficient of 3% H_2O at atmospheric pressure and room temperature is also plotted in figure 1 for comparison. In this work, we select the SF_6 absorption peak centered at 947.89 cm^{-1}. The spectral interference of ambient water is negligible due to its much smaller absorption coefficient and good separation from a targeted SF_6 absorption feature.

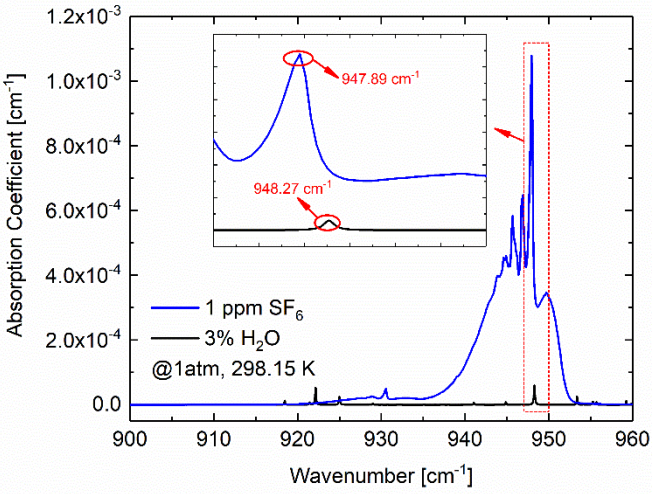

Figure 1. Simulated absorption coefficient of 1 ppm SF_6 and 3% H_2O at 1 atm and 298.15 K based on the HITRAN database [30]. Inset: the selected absorption peak of SF_6 at 947.89 cm^{-1}.

Figure 2 depicts the schematic of the QEPAS-based SF_6 sensor using a 10.5 µm cw DFB-QCL (Alpes Lasers) with an emission power of 9 mW. The laser wavelength was tuned by a low-noise laser driver (Wavelength Electronics). A custom-designed acoustic detection module (ADM)

consists of two wedged ZnSe windows for optical access, as well as a QTF for acoustic detection and two adjacent micro-resonator (mR) tubes (L = 4.4 mm, ID = 0.9 mm) for acoustic amplification. The compact ADM has a size of 3 cm x 3 cm x 1.6 cm that provides a gas sampling volume of only 2.5 mL. We performed the on-beam QEPAS detection and more details can be found in our recent study [31]. Two ZnSe plano-convex lenses (focal length f_1 = 40 mm, f_2 = 20 mm) placed in front of the ADM were used to direct the QCL beam through the mR tubes and the gap (300 µm) between the QTF prongs. A sinusoidal dither at half of the QTF resonant frequency (f_0 ≈ 32.75 kHz) was applied to the laser injection current to generate an acoustic wave at f_0. The acoustic signal was transduced to electrical charges by the piezoelectric vibration of the QTF, and then amplified by a transimpedance preamplifier with a 10-MΩ feedback resistor. The electrical signal was then demodulated by a digital lock-in amplifier to obtain the 2f component for concentration analysis.

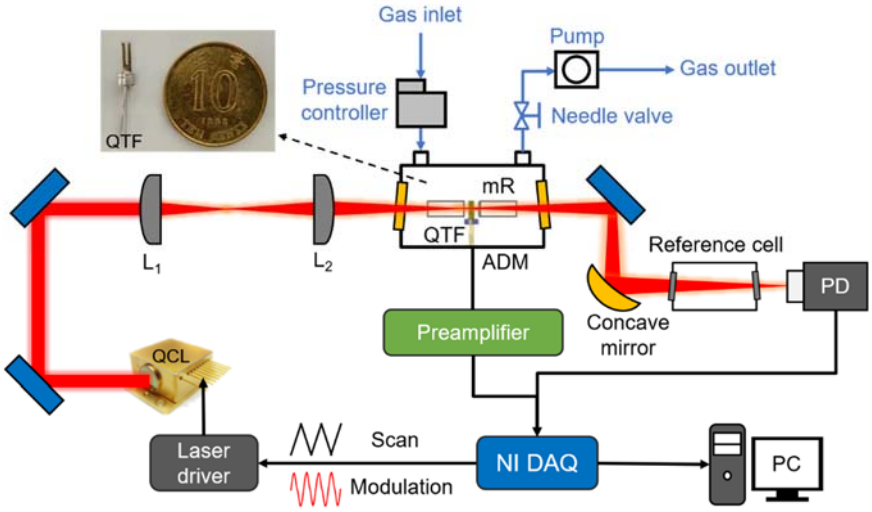

Figure 2. Schematic of the QEPAS-based SF_6 sensor. QCL, quantum cascade laser; L_1 and L_2, plano-convex lenses; ADM, acoustic detection module; QTF, quartz tuning fork; mR, micro-resonator; PD, photodetector; DAQ, data acquisition card.

To implement the wavelength stabilization method, the QCL beam was directed through a 3-cm long reference cell filled with 1% SF_6 at a pressure of 60 torr and finally focused on a low-cost, room-temperature HgCdTe (MCT) photodetector (VIGO Systems, PVM-10.6). The photodetector signal was demodulated by another digital lock-in amplifier at the 3f that acts as an error signal to lock the laser wavelength to the line-center of the absorption feature via a proportional-integral-derivative (PID) control. Note that the function generator, digital lock-in amplifier and

the PID module were all integrated with a LabVIEW-based program to simplify the sensor system for field measurements.

The gas sample was introduced into the ADM for concentration measurements by a diaphragm pump (KNF). A forward pressure controller (Bronkhorst, P-600 series) combined with a needle valve was used to control the gas pressure and flow rate inside the ADM and thus reduced the possible noise caused by pressure fluctuations during the continuous air sampling. All the measurements were conducted at atmospheric pressure (760 torr) and room temperature (25 °C). The QTF used in this work has a Q-factor of 8200 and a resonant frequency of 32.75 kHz. The entire sensing system was designed with a compact size of 30 cm × 30 cm × 19 cm for the purpose of portability.

3. Results and discussion

3.1 Sensor performance

We first scanned the QCL wavelength across the SF_6 spectral feature by superimposing a 0.1-Hz sawtooth waveform on the high-frequency sinusoidal modulation (~ 16.4 kHz). Figure 3 depicts the representative 2f and 3f signals of QEPAS measurements. The 3f component of the absorption measurement of SF_6 in the reference gas cell was then used as the error signal to compensate for any wavelength drift of the QCL [27]. As a result, the laser wavelength was fixed at the absorption peak of SF_6 using a PID feedback loop for the injection current.

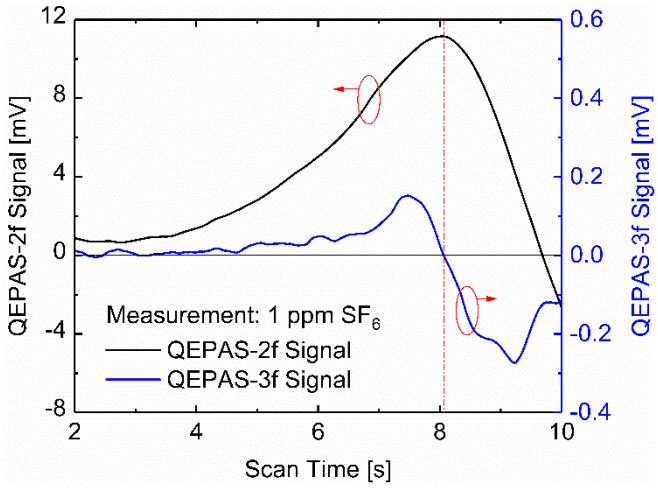

Figure 3. Representative 2f and 3f signals of QEPAS measurements.

Figure 4 illustrates the continuous laboratory measurement of the amplitude of 3f signal with and without the PID control. The 3f logging time by the LabVIEW program was set to be 0.4 s. When the laser was operated at the free-running mode without any PID feedback to its injection current, the 3f signal shows an evident drift during the measurement time of 20 minutes. In comparison, the implementation of PID control calibrated the laser wavelength in real-time and reduced the fluctuations. We believe that wavelength stabilization is required to effectively improve the sensor accuracy and stability in field tests where there may exist significant temperature variations or mechanical vibrations.

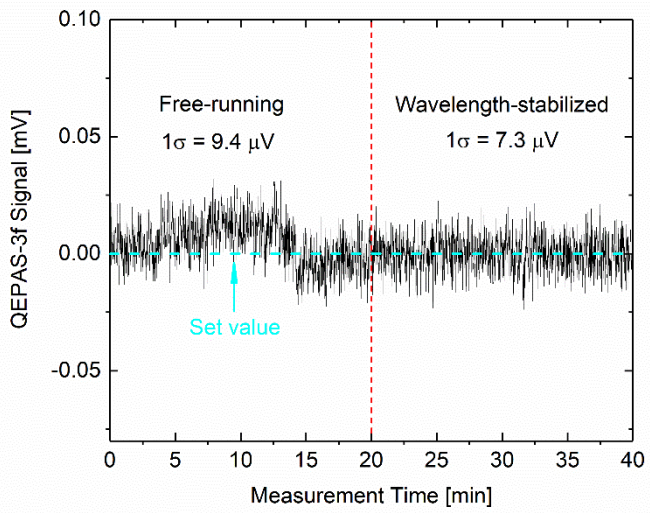

Figure 4. Measured QEPAS-3f signals with the QCL operated at the free-running mode (before 20 minutes) and wavelength-stabilized mode (after 20 minutes), respectively.

After locking the laser wavelength to the target absorption feature, the optimum signal averaging time of the current QEPAS sensor was investigated at different 3f logging intervals. Figure 5 plots the measured QEPAS-2f amplitude of 2.7 ppm SF_6 as a function of 3f logging interval ranging from 0.3 s to 4 s. The minimal averaging time of the sensor was identified to be 0.4 s, below which the QEPAS-2f amplitude starts to decrease. Hence, all the measurements were conducted with an integration time of 0.4 s for the current SF_6 sensor development.

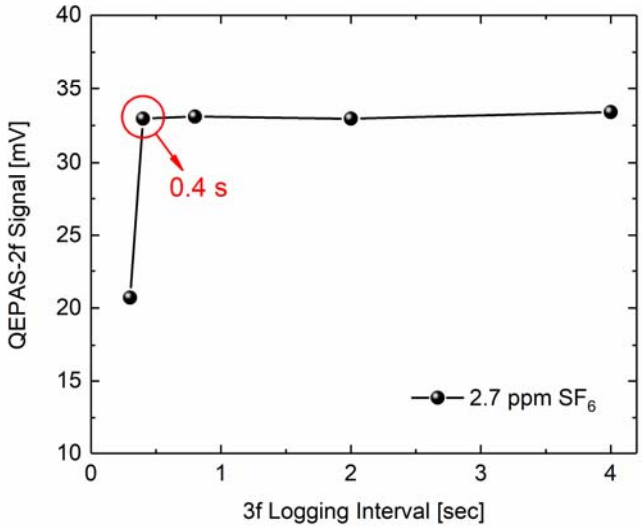

Figure 5. Variation of QEPAS measurement with the 3f logging interval.

The response characteristics of the current SF_6 sensor were investigated by performing gas loading experiments. Here the response time is defined by t_{90}, which is the amount of time that it takes for the gas sensor to reach 90% of the final signal level for a step input [32]. The inlet PFA tube before the ADM has a length of 157 cm and an inner diameter of 4.35 mm, which occupies a volume of ~23 mL. The ADM and all the connecting tubes were first purged by ambient air, and then at the test time of 42 s a sample of 5.9 ppm SF_6 was continuously pumped into the ADM. The entire loading process was monitored by the gas sensor with a time interval of 0.4 s. Figure 6 presents all the QEPAS measurements with the gas flow rate varied between 27 mL/min and 793 mL/min. It is evident shown in Figure 6(a) that all the measurements reach the same plateau level even when the flow rate is as low as 27 mL/min, which indicates negligible surface effects such as the adsorption-desorption process occurred on the cell and tube walls [33]. Hence, the response time of the current SF_6 sensor is determined by the gas diffusion in the inlet tube and the gas exchange in the ADM. In this study, we obtained a response time of 2.8 s at a flow rate of 550 mL/min as illustrated in Figure 6(b); in fact, the much larger volume of the inlet tube (23 mL) dominates the sensor response time. Note that the possible dead volume in the gas sensing system could also be a factor that influences the response time [32,34]. Hence, future work will involve the optimal design of the ADM and the inlet tube.

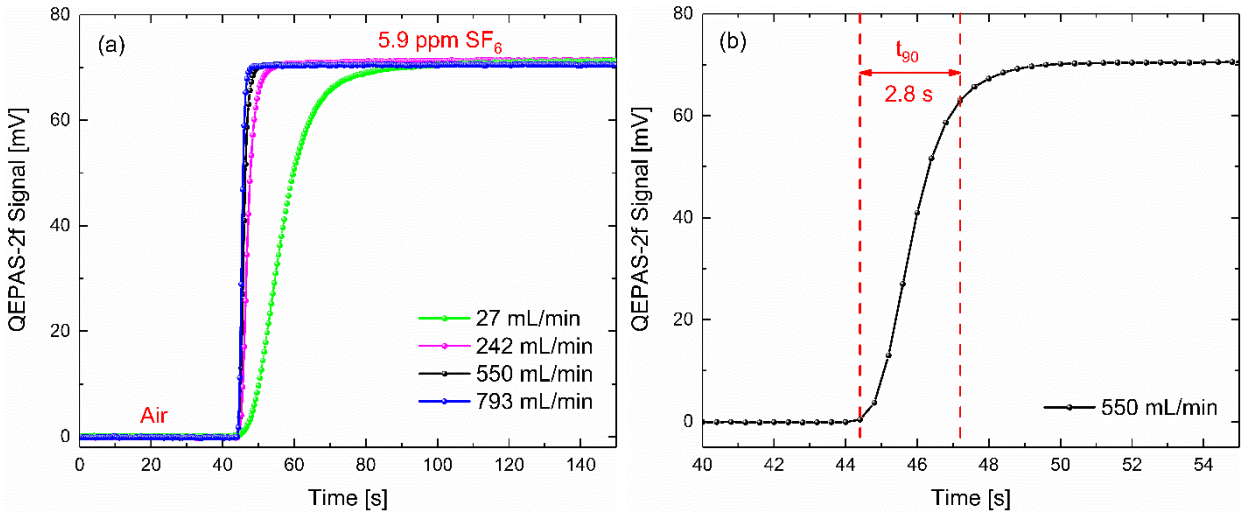

Figure 6. (a) Measured sensor responses when 5.9 ppm SF_6 is loaded into the ADM with different flow rates. (b) Determination of the response time (t_{90}) at the flow rate of 550 mL/min.

The sensor calibration was performed by pumping SF_6 mixtures with known concentrations into the ADM. The gas mixtures were generated by diluting the certified 1% SF_6/N_2 mixture using a gas dilution system (JW-3000, Jinwei Electronics) followed by two mass flow controllers (MFCs) for the further dilution. The measured QEPAS signal as a function of SF_6 concentration is plotted in Figure 7. A linear fit of the experimental data with an R-square value of 0.9996 indicates very good linearity of the sensor. With the obtained standard deviation (1σ) of 56 μV for 0.26 ppm SF_6 over 10-minute measurements, a minimum detection limit (MDL) of 4.6 ppb SF_6 is obtained at 0.4-s integration time based on the fitting curve (12.1 mV/ppm). It should be noted that an improved detection limit could be obtained at longer 3f recording times.

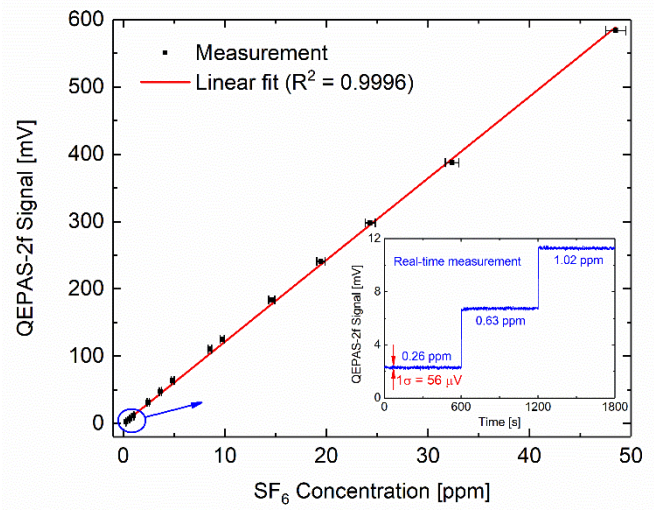

Figure 7. Measured QEPAS-2f signal as a function of SF_6 concentration. The uncertainties in SF_6 concentrations are mainly from the gas dilution system, mass flow controllers, and the certified gas cylinder. Inset: continuous SF_6 measurement using the wavelength-stabilized QEPAS sensor at 0.4-s integration time.

3.2 Field test

The tracer gas concentration decay method is the most widely used method for measuring AERs due to its simple implementation and the minimum demand for the amount of tracer gas [12,13]. Based on the SF_6 tracer technique adopted in this study, it is possible to solve Equation (1) and obtain the corresponding solution:

$$C(t) = C(0)e^{-Nt} . \quad (2)$$

The experiment was then conducted by measuring the indoor SF_6 concentration over a period of time, so that the AER can be obtained using the regression method [35]. To demonstrate the applicability of the QEPAS sensor for ventilation studies, the sensor setup was moved to a testing laboratory for measuring AERs using the SF_6 tracer technique. The testing laboratory shown in Figure 8(a) is located in a compartment of the Indoor Environmental Quality Laboratory at The Hong Kong Polytechnic University.

At the beginning of each test, all the windows and the door were closed. A small amount of 1% SF_6 was released to the testing laboratory. Meanwhile, two electrical fans placed at the diagonal corners of the laboratory were turned on to guarantee a good mixing of SF_6 with the indoor air. The indoor air was continuously sampled by the detection module for concentration measurement at a flow rate of 550 mL/min. The performance of the developed sensor was compared with the commercial gas monitor (B&K 1302) that has a time resolution of ~ 42 s and a detection limit of 5 ppb. Two sampling ports were located 1.7 m above the floor and separated by a horizontal distance of 37 cm.

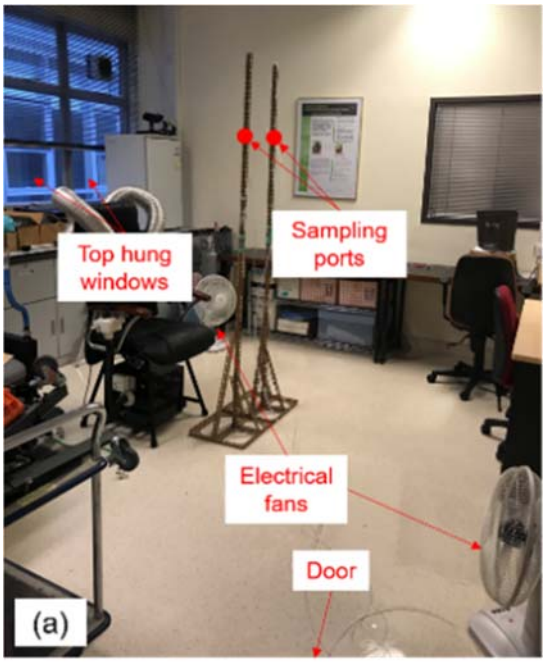
Top hung windows
Sampling ports
Electrical fans
Door
(a)

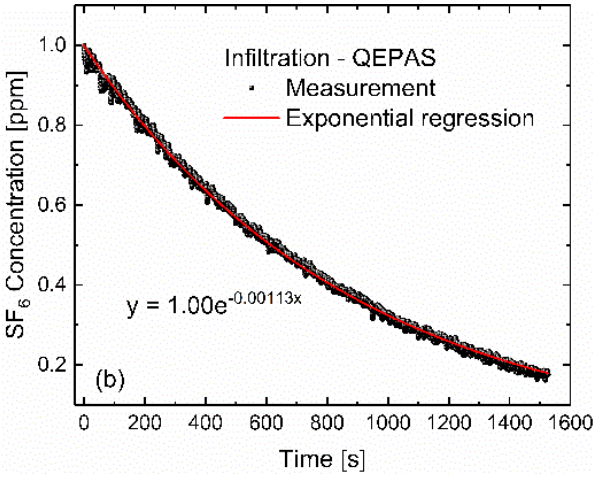
Infiltration - QEPAS
Measurement
Exponential regression
y = 1.00e-0.00113x
(b)
SF6 Concentration [ppm]
Time [s]
1.0
0.8
0.6
0.4
0.2
0
200
400
600
800
1000
1200
1400
1600

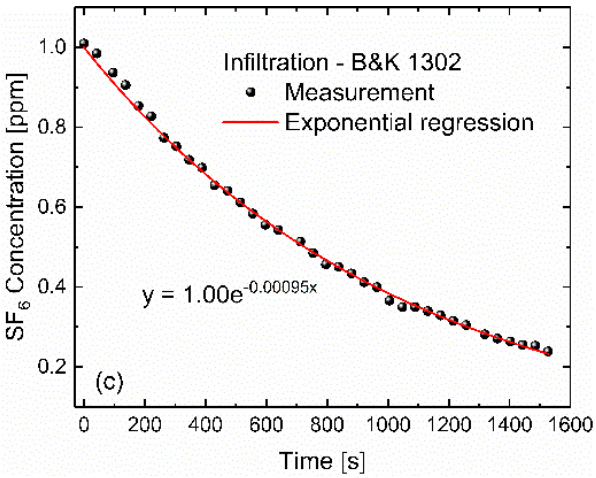
Infiltration - B&K 1302
Measurement
Exponential regression
y = 1.00e-0.00095x
(c)
SF6 Concentration [ppm]
Time [s]
1.0
0.8
0.6
0.4
0.2
0
200
400
600
800
1000
1200
1400
1600

Figure 8. (a) Ventilation testing laboratory. (b) SF_6 concentration decay measurement using the developed QEPAS sensor under the condition of infiltration. (c) SF_6 decay measurement using the commercial analyzer (Bruel & Kjaer 1302).

Two ventilation scenarios were evaluated in this work: 1) infiltration with electrical fans on and all windows/door closed; 2) natural ventilation with the door and two top hung windows open. In the infiltration study, we conducted the SF_6 measurement for 26 minutes to monitor the decay of SF_6 concentration from 1 ppm to the final value of 0.25 ppm. A smooth decay curve was obtained by the QEPAS sensor as indicated in Figure 8(b). We thus obtained an AER of 0.00113 s^{-1} (or 4.07 h^{-1}), indicating that the air filling the room was replaced ~ 4 times by the outdoor air within an hour. Figure 8(c) depicts the simultaneous measurement using the B&K 1302 monitor, showing a similar trend of the decay of SF_6 concentration. The AER was measured to be 3.42 h^{-1} with the possible deviation due to the different sampling sites and imperfect gas mixing in the room. Such a measurement uncertainty was also reported in the other AER measurements even in a fully controlled mechanical ventilated building [36].

For the condition of natural ventilation with the windows and door open, the airflow was mainly driven by natural forces such as wind and thermal buoyancy [12]. Compared with the infiltration, it took less than 5 min for the SF_6 concentration to decrease from 1 ppm to 0.25 ppm, indicating a larger AER under this condition. Figure 9 compares the SF_6 decay measurement under natural ventilation using the QEPAS sensor with that using the B&K 1302 gas monitor. A relatively good agreement is found between these two measurements except for the evident difference in sampling rate. Additionally, the fluctuation of SF_6 concentration was well captured by our QEPAS sensor with a 0.4-s time resolution. Such an unsteady SF_6 concentration during the experiment might be caused by the variation of outdoor meteorological conditions such as temperature and wind velocity. In comparison, the commercial B&K 1302 analyzer only logged seven data points during the measurement period, which is insufficient to capture the transient change of SF_6 concentration and to demonstrate the change of outdoor meteorological conditions.

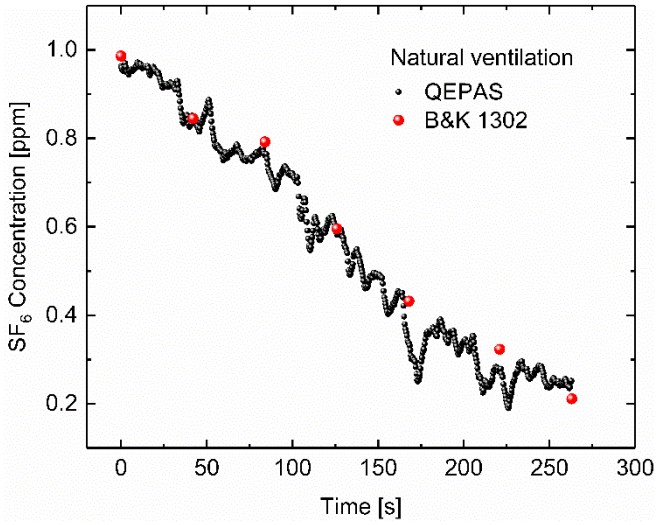

Figure 9. Comparison of the decay measurement of SF_6 concentration using the developed QEPAS and the commercial Bruel & Kjaer 1302 analyzer under the condition of natural ventilation.

4. Conclusion

We have developed a fast-response QEPAS SF_6 sensor for ventilation measurements using a DFB-QCL at 10.5 μm. Wavelength stabilization technique was implemented to achieve a time resolution of 0.4 s and a MDL of 4.6 ppb. The sensor was successfully applied for ventilation rate measurements in a laboratory room using the SF_6 tracer gas concentration decay method. For the infiltration scenario, our measurement agrees well with the commercial B&K 1302 analyzer. For the natural ventilation, the QEPAS-based sensor successfully captured the fluctuation of SF_6 concentration caused by the outdoor meteorological conditions. Future work will involve the implementation of the QEPAS sensor to study the transient contaminant transport, where the contaminant concentration may vary significantly within the test time of a few seconds.

Acknowledgement

This research is supported by the General Research Fund (14206317), the Innovation and Technology Fund (ITS/242/19), the Early Career Scheme (25210419) from the Research Grants Council of the Hong Kong SAR, China, and Natural Science Foundation of Guangdong Province of China (2019A1515011372).

References

[1] Sundell J, Levin H, Nazaroff W W, Cain W S, Fisk W J, Grimsrud D T, Gyntelberg F, Li Y,

Persily A K, Pickering A C, Samet J M, Spengler J D, Taylor S T and Weschler C J 2011 Ventilation rates and health: Multidisciplinary review of the scientific literature *Indoor Air* **21** 191–204

[2] Seltzer J M and Diego S 1994 Building-related illnesses *J Allergy Clin Immunol* **94** 351–61

[3] Charlesworth P S 1988 Air exchange rate and airtigthness measurement techniques- An applications guide. *Build. Serv. Eng. Res. Technol.* **7** 11–8

[4] Pérez-lombard L, Ortiz J, Coronel J F and Maestre I R 2011 A review of HVAC systems requirements in building energy regulations **43** 255–68

[5] Cao G, Awbi H, Yao R, Fan Y, Sirén K, Kosonen R and Zhang J (Jensen) 2014 A review of the performance of different ventilation and airflow distribution systems in buildings *Build. Environ.* **73** 171–86

[6] You R, Zhang Y, Zhao X, Lin C, Wei D, Liu J and Chen Q 2018 An innovative personalized displacement ventilation system for airliner cabins *Build. Environ.* **137** 41–50

[7] You R, Lin C H, Wei D and Chen Q 2019 Evaluating the commercial airliner cabin environment with different air distribution systems *Indoor Air* **29** 840–53

[8] Kiwan A, Berg W, Brunsch R, Özcan S, Müller H J, Gläser M, Fiedler M, Ammon C and Berckmans D 2012 Tracer gas technique, air velocity measurement and natural ventilation method for estimating ventilation rates through naturally ventilated barns *Agric. Eng. Int. CIGR J.* **14** 22–36

[9] Demmers T G M, Phillips V R, Short L S, Burgess L R, Hoxey R P and Wathes C M 2001 Validation of ventilation rate measurement methods and the ammonia emission from naturally ventilated dairy and beef buildings in the United Kingdom *J. Agric. Eng. Res.* **79** 107–16

[10] Blanes V and Pedersen S 2005 Ventilation flow in pig houses measured and calculated by carbon dioxide, moisture and heat balance equations *Biosyst. Eng.* **92** 483–93

[11] Remion G, Moujalled B and El Mankibi M 2019 Experimental characterization of the

impact of unsteady airflows on tracer gas measurement *IOP Conf. Ser. Mater. Sci. Eng.* **609**

[12] Remion G, Moujalled B and El M 2019 Review of tracer gas-based methods for the characterization of natural ventilation performance : Comparative analysis of their accuracy *Build. Environ.* **160** 106180

[13] Cui S, Cohen M, Stabat P and Marchio D 2015 CO_2 tracer gas concentration decay method for measuring air change rate *Build. Environ.* **84** 162–9

[14] Kalliokoski P, Niemelä R, Salmivaara J, Scandinavian S and June N 1980 The tracer gas technique - A useful tool for industrial hygiene *Scand. J. Work. Environ. Health* **6** 123–30

[15] Porter S, Rooney R T and Oestergaard K 2002 An investigation of SF6 gas for testing instrumental integrity of the emerging SULEV/PZEV measurement technology *SAE Tech. Pap. Ser.*

[16] Niemelä R, Lefevre A, Muller J P and Aubertin G 1991 Comparison of three tracer gases for determining ventilation effectiveness and capture efficiency *Ann. Occup. Hyg.* **35** 405–17

[17] Haisch C 2012 Photoacoustic spectroscopy for analytical measurements *Meas. Sci. Technol.* **23** 012001

[18] Kosterev A A, Bakhirkin Y A, Curl R F and Tittel F K 2002 Quartz-enhanced photoacoustic spectroscopy *Opt. Lett.* **27** 1902–4

[19] Patimisco P, Scamarcio G, Tittel F K and Spagnolo V 2014 Quartz-enhanced photoacoustic spectroscopy: A review *Sensors (Switzerland)* **14** 6165–206

[20] Wang Z, Li Z and Ren W 2016 Quartz-enhanced photoacoustic detection of ethylene using a 10.5 μm quantum cascade laser *Opt. Express* **24** 4143–54

[21] Shi C, Wang D, Wang Z, Ma L, Wang Q, Xu K, Chen S C and Ren W 2017 A Mid-Infrared Fiber-Coupled QEPAS Nitric Oxide Sensor for Real-Time Engine Exhaust Monitoring *IEEE Sens. J.* **17** 7418–24

[22] Wang Z, Wang Q, Ching J Y L, Wu J C Y, Zhang G and Ren W 2017 A portable low-power QEPAS-based CO_2 isotope sensor using a fiber-coupled interband cascade laser *Sensors Actuators, B Chem.* **246** 710–5

[23] Jahjah M, Ren W, Stefa´nski P, Lewicki R, Zhang J, Jiang W, Tarkaab J and Tittel F K 2014 A compact QCL based methane and nitrous oxide sensor for environmental and medical applications *Analyst* 2065–9

[24] Kosterev A A, Buerki P R, Dong L, Reed M, Day T and Tittel F K 2010 QEPAS detector for rapid spectral measurements *Appl. Phys. B Lasers Opt.* **100** 173–80

[25] Schilt S, Kosterev A A and Tittel F K 2009 Performance evaluation of a near infrared QEPAS based ethylene sensor *Appl. Phys. B Lasers Opt.* **95** 813–24

[26] Wang G, Yi H, Cai T, Wang L, Tan T, Zhang W and Gao X 2012 Research on the real-time measurement system based on QEPAS *Acta Phys. Sin.* **61** 120701

[27] Wang Q, Wang Z and Ren W 2017 Wavelength-stabilization-based photoacoustic spectroscopy for methane detection *Meas. Sci. Technol.* **28**

[28] Tátrai D, Bozóki Z and Szabó G 2013 Method for wavelength locking of tunable diode lasers based on photoacoustic spectroscopy *Opt. Eng.* **52** 096104

[29] Zhang Q, Chang J, Wang F, Wang Z, Xie Y and Gong W 2018 Improvement in QEPAS system utilizing a second harmonic based wavelength calibration technique *Opt. Commun.* **415** 25–30

[30] Gordon I E, Rothman L S, Hill C, Kochanov R V., Tan Y, Bernath P F, Birk M, Boudon V, Campargue A, Chance K V., Drouin B J, Flaud J M, Gamache R R, Hodges J T, Jacquemart D, Perevalov V I, Perrin A, Shine K P, Smith M A H, Tennyson J, Toon G C, Tran H, Tyuterev V G, Barbe A, Császár A G, Devi V M, Furtenbacher T, Harrison J J, Hartmann J M, Jolly A, Johnson T J, Karman T, Kleiner I, Kyuberis A A, Loos J, Lyulin O M, Massie S T, Mikhailenko S N, Moazzen-Ahmadi N, Müller H S P, Naumenko O V., Nikitin A V., Polyansky O L, Rey M, Rotger M, Sharpe S W, Sung K, Starikova E, Tashkun S A, Auwera J Vander, Wagner G,

Wilzewski J, Wcisło P, Yu S and Zak E J 2017 The HITRAN2016 molecular spectroscopic database *J. Quant. Spectrosc. Radiat. Transf.* **203** 3–69

[31] Wang Z, Geng J and Ren W 2017 Quartz-Enhanced photoacoustic spectroscopy (QEPAS) detection of the v_7 band of ethylene at low pressure with CO_2 interference analysis *Appl. Spectrosc.* **71** 1834–41

[32] Zahn A, Weppner J, Widmann H, Schlote-Holubek K, Burger B, Kühner T and Franke H 2012 A fast and precise chemiluminescence ozone detector for eddy flux and airborne application *Atmos. Meas. Tech.* **5** 363–75

[33] Schmohl A, Miklos A and Hess P 2001 Effects of adsorption–desorption processes on the response time and accuracy of photoacoustic detection of ammonia *Appl. Opt.* **40** 2571

[34] Bozóki Z, Guba T, Ajtai T, Szabó A and Szabó G 2018 Photoacoustic detection based permeation measurements: Case study for separation of the instrument response from the measured physical process *Photoacoustics* **12** 1–5

[35] Sherman M H 1990 Tracer-gas techniques for measuring ventilation in a single zone *Build. Environ.* **25** 365–74

[36] Van Buggenhout S, Van Brecht A, Eren Özcan S, Vranken E, Van Malcot W and Berckmans D 2009 Influence of sampling positions on accuracy of tracer gas measurements in ventilated spaces *Biosyst. Eng.* **104** 216–23